Dynamical Behavior of Carbohydrates As Studied by Carbon-13 and Proton Nuclear Spin Relaxation

Lena Mäler,[†] Göran Widmalm,[‡] and Jozef Kowalewski*,[†]

Division of Physical Chemistry and Department of Organic Chemistry, Arrhenius Laboratory, Stockholm University, S-106 91 Stockholm, Sweden

Received: April 30, 1996; In Final Form: August 24, 1996[⊗]

Variable-field carbon-13 and proton relaxation data are reported for two saccharides: a monosaccharide, 1,6-anhydro-β-D-galactopyranoside; and a disaccharide, methyl 3-*O*-α-D-mannopyranosyl-β-D-glucopyranoside. Carbon-13 measurements were perfomed at two fields, 4.7 and 9.4 T, and at 268, 288, and 303 K for the monosaccharide and at 268, 288, 303, and 323 K for the disaccharide. Proton cross-relaxation measurements were performed at three magnetic field strengths, 7.05, 9.4, and 11.75 T, and at several temperatures, 268, 288, and 303 K for the monosaccharide and 268, 282, 288, and 323 K for the disaccharide. The carbon-13 results were analyzed with the Lipari−Szabo "model-free" approach to obtain estimates of the global correlation times and order parameters. The monosaccharide was found to be very rigid, with $S^2 = 0.91$, while the disaccharide showed some internal motions reflected in a lower order parameter, S^2 around 0.8. The intra-ring proton cross-relaxation could be explained by the motional parameters obtained from the carbon-13 work, yielding reference distances in agreement with molecular modeling for the two molecules. The inter-ring cross-relaxation in the disaccharide was found to display the same field dependence as the intra-ring cross-relaxation, and the same motional paramaters could be used to interpret the inter-ring data. The results indicate that there are no large-amplitude motions on a short time scale around the glycosidic linkage.

Introduction

The motional properties of biomolecules have received considerable attention in recent years.[1−9] A common method for investigating the dynamical behavior of molecular liquids is by means of nuclear spin relaxation. A great deal of work has been done in the field of carbon-13 and nitrogen-15 relaxation measurements on biomolecules. The NMR relaxation parameters indirectly contain dynamical information through the spectral density functions, which can be interpreted within a motional model such as the "model-free" approach taken by Lipari and Szabo.[10] This approach involves the measurement of the common heteronuclear relaxation parameters such as T_1, T_2, and NOE and interpretation of the data in terms of a global, overall molecular correlation time and a set of parameters describing the internal motion. Another approach has beeen taken by Peng and Wagner,[11] who mapped the spectral density functions by conducting measurements of several different relaxation parameters.

In the field of carbohydrate chemistry, molecular dynamics investigations by means of NMR relaxation have frequently been used to establish a picture of the motional properties of oligosaccharides.[12−17] Carbon-13 relaxation studies together with the model-free approach can provide estimates of the overall motion of a molecule together with the parameters determining its possible internal motions.[10,18] The results yield information on the motions modulating the individual carbon−proton vectors in the molecule. From our laboratory we have previously reported carbon-13 relaxation investigations on several systems.[19−22] The dynamics was characterized in terms of a global motion, described by a rather long overall correlation time, and local motions, each described by a short, local correlation time and an order parameter.[20−22] It is possible, however, that there are other types of motions present which could escape carbon-13 relaxation investigations. For example, there might be motions around glycosidic linkages which occur on the time scale of the order of the global correlation time and cannot be separately observed.[23] For studying this type of motion, inter-ring proton cross-relaxation measurements might be an interesting alternative.[10,24] The possibility of motion around glycosidic linkages in oligosaccharides has been the issue of several recent studies, and evidence of such motions has been put forward.[25−30]

In this study we stress the importance of combining accurate carbon-13 determinations with proton measurements. We focus our attention on two related problems. First, we deal with the issue of compatibility of the molecular dynamics from the carbon-13 and proton data, in particular with reference to the Lipari−Szabo model. Second, we apply the approach to investigating the mobility around the glycosidic linkage in a disaccharide. We present a multiple-field carbon-13 relaxation study of one monosaccharide, 1,6-anhydro-β-D-galactopyranoside, and of a disaccharide, methyl 3-*O*-α-D-mannopyranosyl-β-D-glucopyranoside (Figure 1), together with a field- and temperature-dependent proton cross-relaxation investigation. The monosaccharide is believed to be quite rigid and serves as a case where the use of motional parameters obtained by carbon-13 relaxation in the proton study is rather straightforward. The disaccharide contains an α-(1→3) linkage, and it is of interest to see if proton cross-relaxation measurements can provide any additional insight into the possible motions around this linkage as compared to what can be obtained by carbon-13 relaxation measurements.

Theory

The longitudinal relaxation rates (T_1^{-1}) of proton-bearing ^{13}C nuclei are usually dominated by dipole−dipole (DD) relaxation due to directly bonded protons. It is sometimes also necessary

* Author to whom correspondence should be addressed (fax +46 8 152187; e-mail jk@physc.su.se).
[†] Division of Physical Chemistry.
[‡] Department of Organic Chemistry.
[⊗] Abstract published in *Advance ACS Abstracts,* October 1, 1996.

S0022-3654(96)01236-1 CCC: $12.00

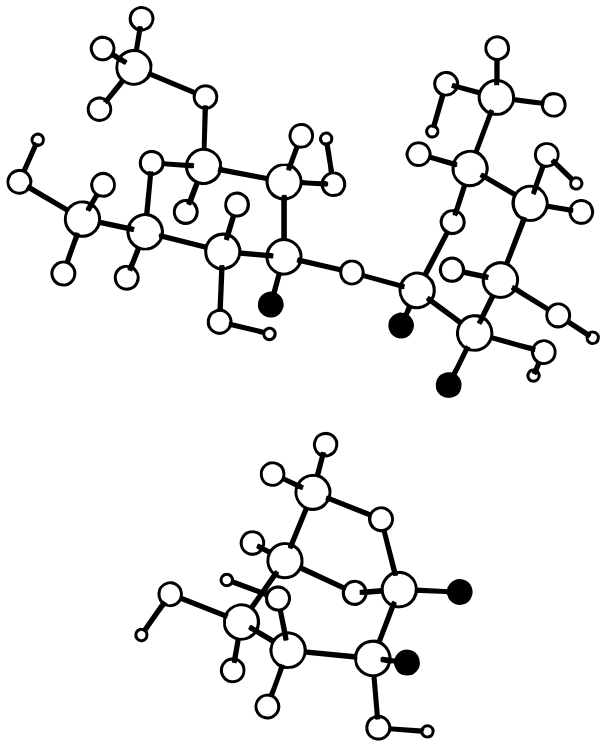

Figure 1. Energy-minimized conformers of the disaccharide α-D-Man*p*-(1→3)-*β*-D-Glc*p*-OMe (a, top) and the monosaccharide 1,6-anhydro-*β*-D-Gal*p* (b, bottom). The solid circles indicate the relevant protons for this study.

to consider chemical shift anisotropy (CSA) as a source of relaxation, in particular in experiments that can be affected by cross-correlation between the two mechanisms.[31] Under broad-band decoupling this effect vanishes, but in the absence of decoupling, schemes for the removal of cross-correlation effects must be employed if quantitative interpretation of the relaxation rates is the goal. Cross-relaxation between the carbon and proton spins under proton decoupling leads to an increase of the steady-state carbon-13 signal intensity by a factor of $1 + \eta$ (the nuclear Overhauser enhancement, NOE). The T_1^{-1} and NOE data can be expressed in terms of spectral density functions taken at combinations of the Larmor frequencies ω_C and ω_H. For carbons carrying one proton, assuming that the relaxation is caused only by the directly bonded proton, the relaxation parameters under investigation here become

$$T_1^{-1} = {}^1/_{10}(\mathrm{DCC})^2[J(\omega_H - \omega_C) + 3J(\omega_C) + 6J(\omega_H + \omega_C)] \quad (1)$$

$$\eta = \left(\frac{\gamma_H}{\gamma_C}\right)\frac{6J(\omega_H + \omega_C) - J(\omega_H - \omega_C)}{J(\omega_H - \omega_C) + 3J(\omega_H + \omega_C) + 6J(\omega_H + \omega_C)} \quad (2)$$

The constant $\mathrm{DCC} = (\mu_0/4\pi)\gamma_C\gamma_H\hbar r_{CH}^{-3}$ is the dipolar coupling constant, related to the dipolar interaction strength between the two nuclei. $J(\omega)$ is the reduced spectral density function. For carbons with two protons attached to them, if one neglects cross-correlation between individual CH vectors, the expressions for T_1^{-1} above should be multiplied by 2 while η stays the same.

To describe the reorientational dynamics of nonrigid molecules in isotropic liquids, the model-free approach of Lipari and Szabo[10] is often used. The reduced spectral density function in this model is composed of two parts, containing a slow global motion and a fast local motion. Assuming that the two motions are statistically independent and that the global motion is isotropic, the spectral density function is given by

$$J(\omega) = \frac{S^2\tau_M}{1 + \omega^2\tau_M^2} + \frac{(1 - S^2)\tau}{1 + \omega^2\tau^2} \quad (3)$$

where $\tau^{-1} = \tau_M^{-1} + \tau_e^{-1}$. τ_M is a correlation time for the global motion, common to the whole molecule, τ_e is the correlation time for a fast local motion, specific for every individual axis in the molecule, and S is a generalized order parameter. S^2 can be defined as the long-time limit of the reorientational time correlation function for the internal motions. The order parameter reflects the spatial restriction of the local motion. If the first term in eq 3 is much larger than the second, eq 3 can be truncated to yield

$$J(\omega) = \frac{S^2\tau_M}{1 + \omega^2\tau_M^2} \quad (4)$$

which is identical to the expression for isotropical small-step diffusion with an amplitude scaling factor S^2.

The proton relaxation in organic molecules is usually a complicated process, involving a large number of different dipole−dipole interactions. The parameter that is suitable for quantitative interpretation is the cross-relaxation rate, σ_{ij}, describing the transfer of magnetization between a given pair of protons i and j, relaxing each other through a dipolar interaction. The cross-relaxation rate is given by the following expression, containing the spectral density functions taken at the sum and difference of the two proton Larmor frequencies:

$$\sigma_{ij} = {}^1/_{10}(\mu_0/4\pi)^2\hbar^2\gamma_H^4\langle r_{ij}^{-6}\rangle[6J^*(2\omega_H) - J^*(0)] \quad (5)$$

Again, $J^*(\omega)$ is the reduced spectral density function, which is here put into the form

$$J^*(\omega) = \frac{S^{*2}\tau_M}{1 + \omega^2\tau_M^2} + (1 - S^{*2})\frac{\tau}{1 + \omega^2\tau^2} \quad (6)$$

where the order parameter squared, S^{*2}, now reflects the effect of internal motions averaging the angular as well as radial part of the dipolar interaction.[10] The other symbols have the same meaning as in eq 3. To a good approximation, S^{*2} can be written as a product of a radial factor $\langle r_{ij}^{-3}\rangle^2/\langle r_{ij}^{-6}\rangle$ and an angular factor defined in analogy with S^2 above.[32] If the internuclear distance is considered to be constant, the radial factor is equal to unity and the definitions of spectral densities in eqs 3 and 6 become identical. If, on the other hand, the internal motions lead to fluctuations of internuclear distances, the meaning of S^{*2} is not the same as S^2 and the spectral densities determining the hetero- and the homonuclear relaxation are different.

Before we leave the theory section, it might be worthwhile to make an additional, fairly trivial comment on the dependence of the dipolar relaxation rates, on the one hand, on the internuclear distances and, on the other hand, on the correlation times. The internuclear distances enter the rate expressions in the sixth power, while the dependence on the correlations times is only linear. Thus, if a certain discrepancy between two rate parameters needs to be rationalized, the numerical outcome will be different if we explain it in terms of a change in a distance or in dynamics. For example, a 25% percent change in a cross-relaxation rate implies a 25% change in the correlation time at

assumed constant distance. If one chooses to explain the same rate change in the σ_{ij} in terms of a modified internuclear distance, a change of r_{ij} by 4% only is sufficient.

Experimental Section

The monosaccharide 1,6-anhydro-β-D-galactopyranoside and the disaccharide α-D-Man*p*-(1→3)-β-D-Glc*p*-OMe were dissolved in a 7:3 molar ratio mixture of D_2O−DMSO-d_6 to yield 100 mM solutions. In the disaccharide, primed labels refer to the mannopyranosyl group and the unprimed to the methyl glucoside residue. The disaccharide has been synthesized and the NMR spectrum assigned previously.[33] The mixed solvent was chosen for its high viscosity and good cryogenic properties, enabling measurements outside the extreme narrowing regime. In a previous study,[34] using the same cryosolvent, the possible influence of the significant amount of DMSO present in the solvent was investigated by performing NOESY experiments in D_2O and in the mixed solvent. From NOE buildup, it was concluded that no significant change in interglycosidic distances could be observed. Thus, one does not anticipate large changes in conformation of the disaccharide in the cryosolvent as compared to D_2O. The samples were transferred to 5 mm NMR tubes that were flame-sealed under vacuum after several freeze−pump−thaw cycles. Carbon-13 relaxation measurements were performed at two magnetic fields using a Bruker MSL 200 operating at 4.7 T and a JEOL Alpha 400 operating at 9.4 T. Fast inversion−recovery experiments[35] were used to measure T_1 values, and the dynamic NOE sequence[36] was employed for the NOE measurements. The heteronuclear NOEs were obtained by taking the ratio between the peak intensities from one experiment with a long irradiation period ($>5 \times T_1$) and another with a short irradiation period (1 ms). The errors in the T_1 values are estimated to be <5%, and the accuracy in the NOE factor is better than 0.1. Carbon-13 relaxation was measured at 268, 288, and 303 K for the monosaccharide and at 268, 288, 303, and 323 K for the disaccharide. Cross-relaxation experiments were perfomed at three magnetic fields, using the following spectrometers: Varian U300 (7.05 T), JEOL Alpha 400 (9.4 T), and Varian U500 (11.85 T). For the monosaccharide, measurements were performed at 268, 288, and 303 K and for the disaccharide, at 268, 282, 288, and 323 K. The proton−proton cross-relaxation rates were measured with the 1D-NOESY pulse sequence proposed by Kessler *et al.*,[37,38] with the selective excitation obtained with a half-Gaussian-shaped pulse[38] of approximately 50 ms duration. In the monosaccharide, the anomeric proton H1 was selectively excited, and the cross-relaxation buildup to H2 was observed. For the disaccharide, the cross-relaxation buildup was monitored from H1′ to the neighboring H2′ and transglycosidically to the H3. Series of 12−20 spectra with different τ_m values were recorded, with τ_m ranging from 1 ms to 8 s for the monosaccharide and from 1 ms to 4 s for the disaccharide. Special care was taken to obtain spectra at short mixing times so that the cross-relaxation rate, σ_{ij}, could be determined from the linear extrapolation of the intensties to zero mixing time (initial rate approximation);[39] 128−512 transients were recorded for every mixing time. The waiting period was typically 10−16 s. Examples of the experimental buildup curves are presented in Figure 2 for the monosaccharide and in Figures 3 and 4 for the disaccharide. Standard temperature-control equipment provided by the manufacturers was used, and the temperature was calibrated with a methanol shift thermometer. Internal deuterium lock was used for field/frequency stabilization. All experiments at 4.7 and 9.4 T were performed twice, and some of the experiments at the other fields were also repeated twice. The average values from the individual experiments are reported. Model building and energy minimization for the two molecules were performed with Quanta/CHARMm, version 4.0 (Molecular Simulations Inc., Burlington, MA).

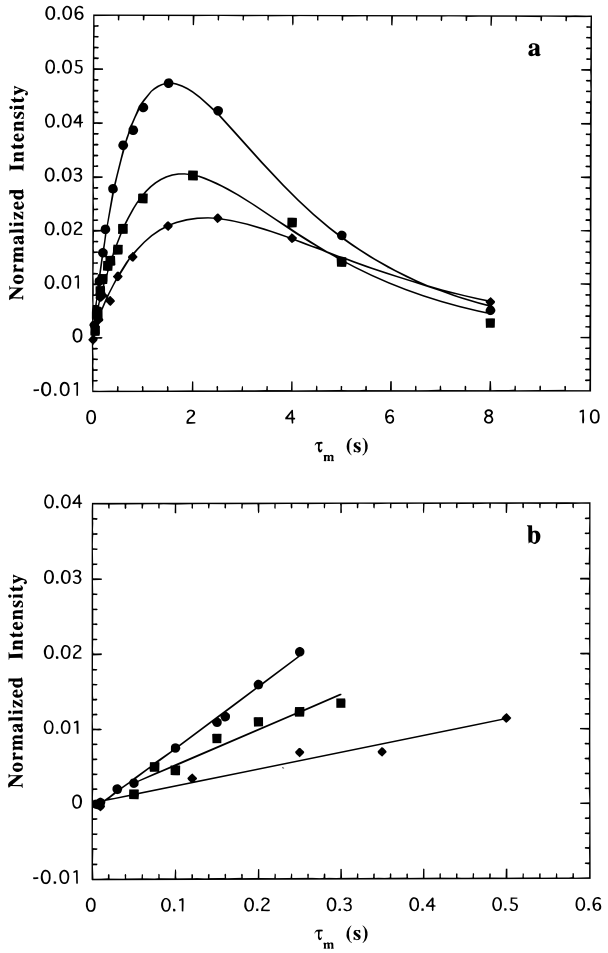

Figure 2. Cross-relaxation buildup between H1 and H2 in the monosaccharide at 268 K, obtained by selectively irradiating H1: (a) whole curves; (b) expansion of the linear region used for determining the cross-relaxation rates, σ. Circles correspond to 7.05 T, squares to 9.4 T, and diamonds to 11.85 T.

Results and Discussion

As mentioned in the Introduction, the goal of this study is twofold. First, we wish to investigate whether the results of the Lipari−Szabo analysis of the carbon-13 relaxation data are compatible with the measured cross-relaxation rates for intraresidue proton pairs. If this is the case, we can move to the second goal and try to use the interglycosidic proton−proton cross-relaxation rates to probe the flexibility of the glycosidic linkage.

The concept of the flexibility of the glycosidic linkage is related to the conformational properties of the oligosaccharide and may require some clarifying comments. Molecular modeling[23] and *ab initio* quantum chemistry[40] studies indicate that the conformational maps of the α-linked disaccharides display multiple minima, some of them separated by low barriers. The conformation analysis—trying to establish the occurrence and populations of different conformers—is not the purpose of this study. Instead, we are concentrating on obtaining information on the shape of the conformational map in the vicinity of the minimum (or minima). More specifically, we try to use experimental data to answer questions such as the following: How extensive is the conformationally accessible space? If more than one conformation is accessible, are there any substantial barriers?

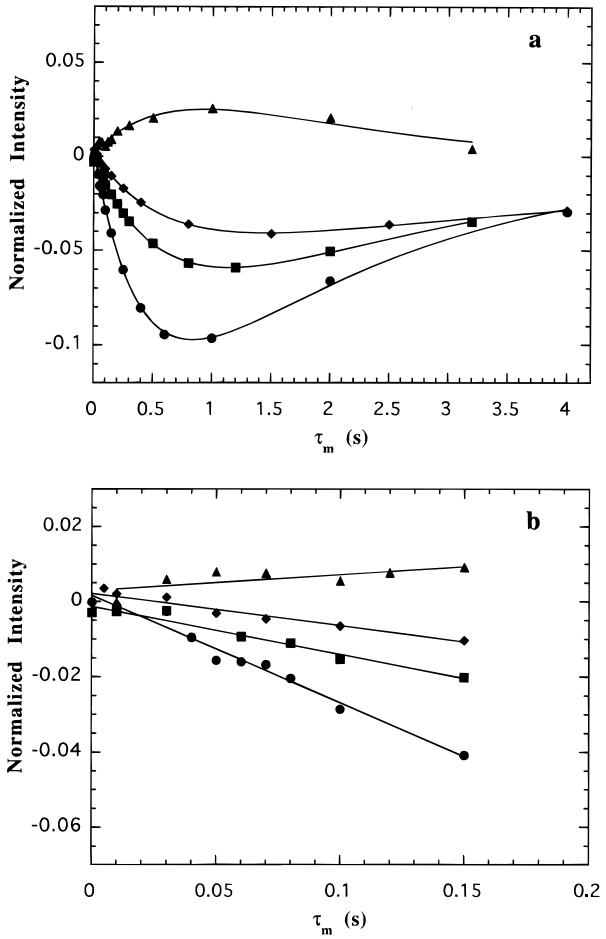

Figure 3. Cross-relaxation buildup between H1′ and H2′ in the disaccharide at 9.4 T, obtained by selectively irradiating H1′: (a) whole curves; (b) expansion of the linear region used for determining the cross-relaxation rates, σ. Circles correspond to 268 K, squares to 282 K, diamonds to 288 K, and triangles to 323 K.

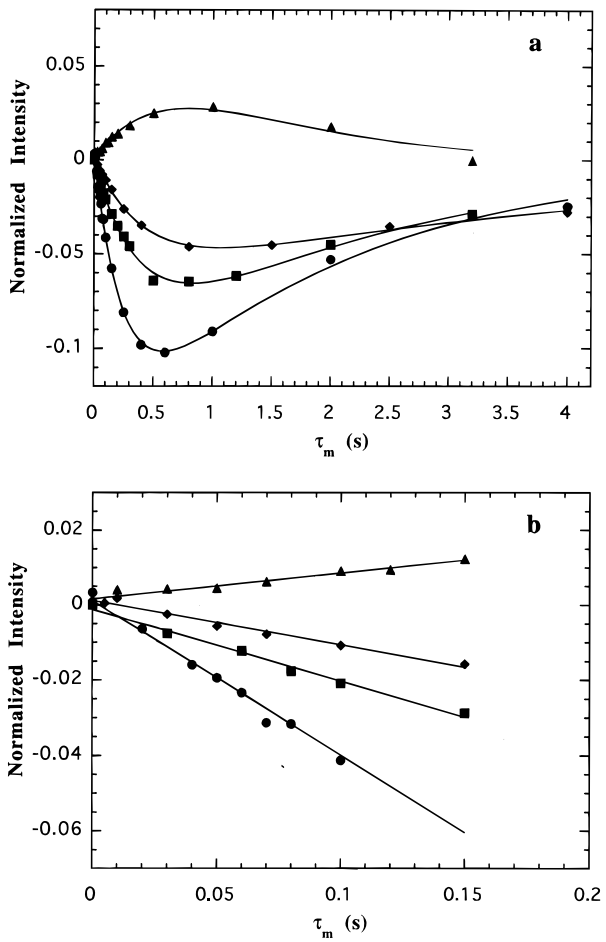

Figure 4. Cross-relaxation buildup between H1′ and H3 in the disaccharide at 9.4 T, obtained by selectively irradiating H1′: (a) whole curves; (b) expansion of the linear region used for determining the cross-relaxation rates, σ. Circles correspond to 268 K, squares to 282 K, diamonds to 288 K, and triangles to 323 K.

Carbon-13 Relaxation. Carbon-13 relaxation was measured for all ring carbons in the monosaccharide and for all well-resolved ring carbon signals in the disaccharide. The carbon-13 relaxation data were interpreted with the Lipari and Szabo model-free approach.[10] For the monosaccharide 1,6-anhydro-β-D-galactopyranoside, only measurements at 268 K showed that the motion was clearly outside the extreme narrowing region (the extreme narrowing regime is defined as $\omega_k\tau_c \ll 1$ for all relevant frequencies ω_k and correlation times τ_c; relaxation parameters in the extreme narrowing limit are independent of the applied magnetic field). For the disaccharide methyl 3-*O*-α-D-mannopyranosyl-β-D-glucopyranoside, however, field-dependent data were obtained at all temperatures. The relaxation parameters for this molecule at 9.4 T and 288 and 303 K are given in Table 1. We can see that the parameters for the individual carbons in the molecule are similar. At 303 K, the relaxation times for the carbons in the terminal mannose residue are slightly shorter than for the carbons in the *O*-methylglucose residue. This might indicate anisotropy of the motion, but the difference is too small to give a quantitative difference in the motional parameters (we analyzed the rings individually, but the differences in the obtained parameters were smaller than the estimated errors). In the following we thus assume the motion to be isotropic and analyze the relaxation data of the disaccharide at each temperature by applying a two-parameter fit, optimizing τ_M and S^2 while setting $\tau_e = 0$. In practice, this fit is equivalent to fitting the data to the truncated form of the Lipari−Szabo model (eq 4). The use of the truncated form is justified since the order parameters were found to be too high to allow accurate determination of the local correlation time, as has been demonstrated previously in several other carbohydrates.[20−22] In the study of the linear tetrasaccharide lacto-*N*-neotetraose,[20] the two central sugar residues had an order parameter squared of around 0.8, and for those residues it was not possible to determine the local correlation time. For the outer rings, however, where the order parameter was lower ($S^2 \approx 0.6$), a local correlation time of around 100 ps could be determined. Thus, we found the order parameters for the two molecules in this study to be high enough to render the second term in the Lipari−Szabo equation negligible.

TABLE 1: Relaxation Parameters Obtained for the Disaccharide α-D-Man*p*-(1→3)-β-D-Glc*p*-OMe at 9.4 T and at Two Temperatures, 288 and 303 K

	288 K		303 K	
carbon	T_1 (ms)	1 + NOE	T_1 (ms)	1 + NOE
C-1	240	1.22	280	2.25
C-2	232	1.16	273	2.10
C-3	221	1.13	262	2.25
C-5	221	1.20	270	2.11
C-1′	217	1.23	256	2.18
C-4′	239	1.14	240	2.10
C-5′	230	1.20	241	2.15

The results of the fits for the disaccharide are collected in Table 2. When examining these results, we see clearly that the global correlation time increases with decreasing temperature, while the order parameter squared shows almost no

TABLE 2: Motional Parameters for the Disaccharide α-D-Man*p*-(1→3)-*β*-D-Glc*p*-OMe Obtained by a Two-Parameter Least-Squares Fit of the Ring Carbon Relaxation Parameters to the Truncated Lipari−Szabo Equation (Eq 4)

T (K)	τ_M (ns)	S^2	Δy^a
268	2.19 ± 0.16	0.80 ± 0.02	3.5
288	0.80 ± 0.04	0.81 ± 0.02	3.2
303	0.42 ± 0.04	0.77 ± 0.04	4.4
323	0.21 ± 0.05	0.75 ± 0.15	7.4

[a] Standard deviation of the dependent variable (%).

TABLE 3: Motional Parameters for the Monosaccharide 1,6-Anhydro-*β*-D-Gal*p* Obtained from the Carbon-13 Relaxation Parameters

T (K)	τ_M (ns)	S^{2a}	Δy^b
268	0.200 ± 0.020	0.91± 0.07	2.6
288	0.093 ± 0.002	0.91	3.6
303	0.053 ± 0.001	0.91	2.4

[a] The value at 268 K is obtained by a two-parameter fit; the values at the other temperatures are held constant. [b] Standard deviation of the dependent variable (%).

temperature dependence (0.81−0.75) over the range used in this study. Assuming an Arrhenius temperature dependence according to $\tau_M = \tau_0 \exp(E_a/RT)$ for the global correlation time, τ_M, one obtains an activation energy of 30.8 kJ/mol and a τ_0 of 2.15 fs. These parameters can be used to calculate τ_M at any other temperature, with the assumption of a constant order parameter. The results are in agreement with earlier findings for oligosaccharides of the same size.[20,22] Thus, the introduction of an order parameter S^2 of around 0.8 is sufficient to explain the carbon-13 relaxation data well. This is consistent with a molecule displaying some restricted internal motion, reflected in the order parameter not much less than unity.

A comparison of the flexibility of the present disaccharide with other disaccharides has previously been done by means of energy minimizations,[33] with respect both to their minimum energy conformation and to the available conformational space (Ramachandran maps). A somewhat different degree of flexibility is anticipated to be present in α- and *β*-linked sugars, and indeed, larger conformational freedom was found for the *β*-linked sugars. This is also in agreement with relaxation measurements on oligosaccharides reported from this laboratory[20,41] which show lower S^2 values than in the present α-linked disaccharide.

For the monosaccharide, the data at 268 K were analyzed by the use of the same two-parameter fit as for the disaccharide. This procedure yielded an S^2 of 0.91 and a global correlation time of 0.200 ns, in agreement with a rigid, moderately slowly tumbling molecule. This is to be expected from the almost spherical shape of the molecule (see Figure 1). Because the order parameter is expected to be roughly temperature independent, and using its value at 268 K, we can calculate the global correlation time, τ_M, also at the temperatures where the molecule is near or within the extreme narrowing region. These results are presented in Table 3. Although the carbon-13 relaxation is within the extreme narrowing limit, the proton relaxation may be outside, due to the higher frequencies involved. It is therefore important to determine the dynamical parameters accurately, since an "effective" correlation time $\tau = \tau_M S^2$ might be possible to use in the carbon-13 work, but not in the proton work.

For large molecules, the validity of the assumption of the Lipari−Szabo model concerning the statistical independence of the overall and internal motion is usually ascertained by the time scale separation of the two motions. In the case of the two small sugar molecules of the present work, the global correlation times are not necessarily always much longer than τ_e. This is particularly true for the monosaccharide and for the disaccharide at elevated temperatures. Since the low- and high-temperature data are fully consistent with each other (*vide infra*), we do not believe that this constitutes a serious problem for the purpose of the present study.

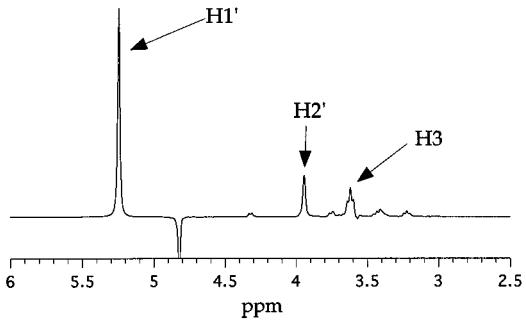

Figure 5. Proton 1D-NOESY spectrum of the disaccharide α-D-Man*p*-(1→3)-*β*-D-Glc*p*-OMe at 9.4 T and $T = 268$ K obtained with the mixing time $\tau_m = 600$ ms. As indicated in the spectrum, the anomeric proton in the mannosyl group was selectively irradiated. The strong negative peak is due to the residual HDO signal.

TABLE 4: Cross-Relaxation Parameters Obtained for the Disaccharide α-D-Man*p*-(1→3)-*β*-D-Glc*p*-OMe

		σ_{ij} (s^{-1})			
proton pair	B_0 (T)	268 K	282 K	288 K	323 K
H1′,H2′	7.05	−0.290	−0.090		0.072
	9.4	−0.290	−0.117	−0.086	0.050
	11.75	−0.308	−0.126		0.030
H1′,H3	7.05	−0.380	−0.145		0.100
	9.4	−0.417	−0.174	−0.119	0.069
	11.75	−0.422	−0.193		0.050

Proton Relaxation. The cross-relaxation rate, σ_{ij}, was evaluated from the buildup curves with the initial rate approximation, i.e. using linear fits of normalized intensities at short mixing times and evaluating σ_{ij} as the slope. For the disaccharide, we analyzed the cross-relaxation buildup of magnetization transfer from the H1′ proton to the neighboring proton in the same ring, H2′, as well as the inter-ring transfer to the proton H3. The transfer of magnetization to other protons was also observed. These NOEs were found to be very small, something that can clearly be seen in the spectrum presented in Figure 5. The evaluation of these small NOEs in terms of distances would yield a high degree of uncertainty. In addition, the transfer of magnetization to more distant protons is sensitive to three-spin effects;[42] furthermore, the conformational analysis of the disaccharide was not the aim of this study. Therefore, we concentrated on the analysis of the large H1′,H2′ and H1′,-H3 cross-relaxation parameters. For the disaccharide, the measurements were performed at several temperatures at each magnetic field. The results are summarized in Table 4. There is a clear field dependence of the parameters corresponding to both the intra- and inter-ring transfers. The data were analyzed according to the following. As the intra-ring cross-relaxation is expected to be due to a dipolar interaction between a proton pair with a "fixed" distance, we assume that the motional parameters determined by the carbon-13 relaxation can be used in connection with eqs 5 and 6 and with $S^{*2} = S^2$ to evaluate a proton−proton distance. The S^2 factors for the carbon−proton and proton−proton interactions are not necessarily equal, even if the interproton distance can be considered constant. Because of the "dynamic equivalence" observed for different carbon−proton bond axes in a single carbohydrate ring,[20−22] one might,

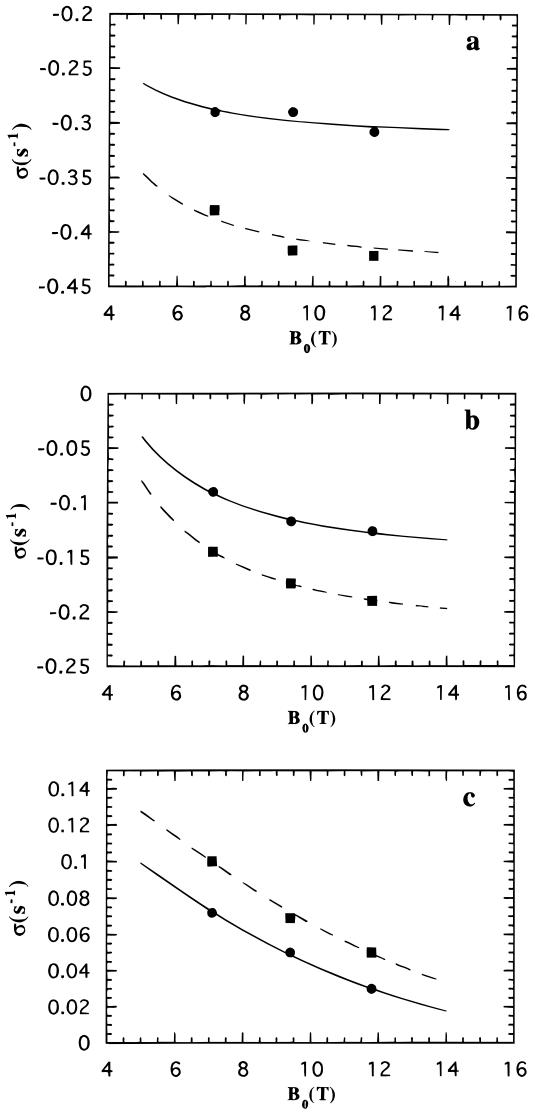

Figure 6. Cross-relaxation parameters, σ, for the disaccharide as a function of the magnetic field at (a) 268, (b) 282, and (c) 323 K. Circles are the experimental points for the cross-relaxation between H1′ and H2′, and squares represent the cross-relaxation between H1′ and H3. The lines represent the best fit to eq 5, using the motional parameters from Table 2.

however, expect this equivalence to extend to the intra-ring proton−proton axes. The distance H1′,H2′ is obtained by a single-parameter least-squares fit of the variable-field data to eq 5 at 268, 282, and 323 K (but not at 288 K since measurements were only perfomed at one field). We obtain the distance H1′,H2′ of 2.62, 2.63, and 2.63 Å at the three different temperatures, respectively. The quality of the fits is illustrated in Figure 6, where the experimental points are compared with the calculated curves. The fact that the distance is temperature independent is satisfying in itself. Furthermore, by performing molecular mechanics energy minimization of the disaccharide, we obtained an estimate of the intra-ring distance, H1′,H2′, of 2.56 Å (Figure 1), which is in satisfactory agreement with the experimental results. It thus seems that the proton relaxation data can be very well interpreted with the Lipari−Szabo parameters from the carbon work; that is, the two approaches are compatible with each other.

We used the same analysis for the monosaccharide. The cross-relaxation rates for this molecule are collected in Table 5. The situation is simpler in this case, since the molecule is quite rigid, which was confirmed by the analysis of the carbon-13 relaxation data (the order parameter squared is around 0.9). Field-dependent data from three different magnetic fields at 268 K were obtained, and we fit the data at this temperature to obtain the distance H1,H2. The errors in the cross-relaxation parameters are judged to be larger than for the disaccharide counterparts, since the measured parameters for the monosaccharide were smaller. However, we obtained a reasonable estimate of the distance as 2.65 Å. At the two higher temperatures, we had only cross-relaxation rates at one and two fields, respectively. Thus, these data were analyzed by simply calculating a distance from each cross-relaxation rate, using the motional parameters from above. The value of this distance was found to be in the range of 2.62−2.65, in agrement with the fit. Again, this should be compared to the geometry of the energy-minimized monosaccharide given in Figure 1, where a distance of 2.55 Å was obtained.

TABLE 5: Cross-Relaxation Parameters Obtained for the Monosaccharide 1,6-Anhydro-*β*-D-Gal*p*

		σ_{ij} (s^{-1})		
proton pair	B_0 (T)	268 K	288 K	303 K
H1,H2	7.05	0.084		
	9.4	0.061	0.051	0.034
	11.75	0.046	0.050	

It is often found in the literature that carbon-13 data cannot provide estimates of correlation times, which can be used in the proton cross-relaxation work to obtain accurate distances.[34,43,44] The problem is often to take the internal motion adequately into account, something that can be demonstated by using an effective correlation time, $S^2\tau_M$, when the proton relaxation data are interpreted. When an effective correlation time from the carbon-13 data is calculated for the disaccharide, neglecting internal motion (in practice setting $S^2 = 1$ in the carbon-13 analysis), one obtains 0.15 ns at 323 K. The correlation times at the two other temperatures can easily be obtained in the same way. If these values are used in the analysis of the proton relaxation data, one obtains a distance H1′,H2′ of 2.60, 2.55, and 2.79 Å for the temperatures 268, 282, and 323 K, respectively. On the other hand, with a reasonable value for the distance H1′,H2′ ($r_{H1',H2'} = 2.62$ Å), the effective correlation time resulting from the proton data at 323 K is twice that obtained from the carbon-13 data (0.29 ns at 323 K), neglecting the internal motions. When internal motions in terms of an order parameter less than unity are introduced, the correlation time $\tau_M = 0.21$ ns is obtained at 323 K both from the carbon-13 data (Table 2) and from proton cross-relaxation data. The apparent discrepancy can thus be explained by the introduction of internal motions described by an order parameter of around 0.8. For the monosaccharide the effect is less dramatic, since the internal motions are more restricted ($S^2 = 0.91$) and the concept of an effective correlation time is more meaningful. When internal motions are present, it is important to stress the need for careful determination of the motional parameters outside the extreme narrowing limit, so as to obtain not only an effective correlation time $S^2\tau_M$ but the two parameters separately. Clearly, the results indicate that internal motions are present in the disaccharide; they can be explained quantitatively by the introduction of an order parameter squared of 0.80.

If both the proton and carbon data are well within the extreme narrowing limit, the use of an effective correlation time, neglecting internal motions, should be sufficient to interpret the data.[45] It is, however, often the case that the carbon relaxation is just within the extreme narrowing limit, making it impossible to determine τ_M and S^2 separately, whereas the proton relaxation is not. The other extreme occurs when τ_M is very long, so that

$(2\omega_H\tau_M)^2 \gg 1$. In this limit, the equation for the cross-relaxation rate becomes

$$\sigma_{ij} = -^1/_{10}(\mu_0/4\pi)^2\hbar^2\gamma_H^4\langle r_{ij}^{-6}\rangle S^{*2}\tau_M \qquad (7)$$

where the field dependence again vanishes.[45] If the measurements are carried out near one of the extremes, it is very difficult to determine the motional parameters correctly, which in turn may lead to misinterpretation of relaxation results. There is in principle nothing novel in this reasoning, but we want to emphasize the advantages of using the field-dependent relaxation data for the evaluation of dynamical parameters.

We now turn to the transglycosidic, inter-ring cross-relaxation of the H1′,H3 proton pair. The behavior of this cross-relaxation rate may carry information on rapid local motion around the glycosidic linkage in a disaccharide. If such motions are absent and if the two rings are dynamically equivalent, the inter-ring cross-relaxation should be determined by the same spectral densities as in the intra-ring case. In the presence of a rapid local motion around the glycosidic linkage, the spectral densities for the intra- and inter-ring dipolar interactions should differ. The difference in the spectral density functions will result in different field dependencies for different cross-relaxation rates. The cross-relaxation rates for the H1′,H3 proton pair in the disaccharide were analyzed in a manner similar to the procedure used for the intraresidue proton pair. If it is indeed the case that the field dependence of this rate is the same as for the intra-ring proton pair, then the reduced spectral densities and the motional parameters should be the same for both proton pairs, i.e. H1′,H2′ and H1′,H3. When examining the data of Table 4, one can note that the ratio between $\sigma_{H1',H2'}$ (500 MHz) and $\sigma_{H1',H2'}$ (300 MHz) (1.1, 1.4, and 0.4)—a simple single-parameter indicator of the field dependence—at the three temperatures, 268, 282, and 323 K, attains roughly the same values as the ratio of $\sigma_{H1',H3}$ (500 MHz) and $\sigma_{H1',H3}$ (300 MHz) (1.1, 1.3, and 0.5) at the same temperatures. It is also worth noting that the field dependence at the lowest temperature is very weak, indicating that the need to separate the order parameter form the correlation time is not very strong and that one could approximately use eq 7 to calculate the distance. At this temperature, this indeed proved to be the case as the $r_{H1',H2'}$ calculated with $S^2 = 1$ (2.60 Å) did not differ much from what was obtained from the fit (2.62 Å) with the carbon-13 motional parameters. As the field dependence for the two proton pairs was found to be almost the same, we attempted to treat the inter-ring data in the same way as the intra-ring results, i.e. to fit the distance H1′,H3 at each temperature using the motional parameters from the carbon-13 results. This resulted in distances of 2.48, 2.45, and 2.48 Å for the three temperatures. The quality of the fits can be seen together with those for the H1′,H2′ proton pair in Figure 6. This distance is shorter than the H1′,H2′ distance; a comparison with molecular modeling indicates that this is reasonable. The low-energy conformer in Figure 1a shows an H1′,H3 distance of 2.34 Å, and the dihedral angles φ_H and ψ_H, defined as H1′−C1′−O3−C3 and C1′−O3−C3−H3′, are equal to −38° and 55°, respectively. A previous energy minimization, using a different force field[33] (the HSEA force field), gave a conformer with $\varphi_H = -40°$ and $\psi_H = -20°$. The interresidue distance H1′,H3 was in this case 2.40 Å. It should be pointed out, as discussed under Theory, that the comparison of the distances should be made with great care: a small change in the distance corresponds to a much larger change in the cross-relaxation parameter, since the distance goes as r^{-6} in eq 5. The reasonable distance obtained in the fits using the ^{13}C dynamical parameters is thus judged as an indication of the lack of high-amplitude motions around the glycosidic linkage, while the similarity of the field dependence of the cross-relaxation rates for the intra- and interresidue proton pairs provides a stronger evidence.

The difference in the distances obtained at different temperatures is for the H1′,H3 proton pair larger than for the H1′,H2′ proton pair but is still not large enough to give rise to any speculations on additional motion as compared to what was found for the intraresidue proton pair. Additional internal motion for the inter-ring proton pair should be reflected in a lower order parameter. Therefore, we also repeated the calculations using somewhat lower values of the order parameter in the fit; this led to even larger differences between the distances obtained at different temperatures. The motional parameters that best explain the proton data are thus consistent with the results of the carbon-13 analysis. Contrary to what has been reported for sucrose[25] and for two other disaccharides,[26] in α-D-Man*p*-(1→3)-*β*-D-Glc*p*-OMe we can see no difference in field-dependent or temperature-dependent behavior of the cross-relaxation buildup of magnetization between the intra-ring case and the inter-ring case.

In a recent molecular dynamics simulation study of a disaccharide,[23] the Lipari−Szabo model-free order parameter, S^2, was obtained for various proton pairs from the dynamics trajectories where overall rotational and translational motions had been removed. Using two different force fields and two different dielectric constants, it was observed that S^2 values for transglycosidic proton pairs were normally lower than those for vicinal intraresidue pairs. This fact, together with differences in radial averaging, i.e. $\langle r^{-3}\rangle^2$ versus $\langle r^{-6}\rangle$, should make it possible to observe different relaxation behavior for the interresidue H1′,H3 and the intraresidue H1′,H2′ proton pairs for certain conformational averaging processes.

We now turn back to the questions proposed in the beginning of this section related to the conformationally accessible space. The parameters for the internal motion in the Lipari−Szabo model, S and τ_e, can be related to the parameters θ_0 and D_w in the diffusion in the cone model.[46] The parameter θ_0 is the angle at the maximum amplitude of the motion, i.e. the semiangle of a cone within which the local motion is restricted, and D_w is the "wobbling" diffusion coefficient. The following expression relates the angle, θ_0, to the Lipari−Szabo order parameter S:

$$\cos\theta_0 = {}^1/_2[(1 + 8S)^{1/2} - 1] \qquad (8)$$

With $S^2 = 0.78$ (averaged over the different temperatures) for the interresidue proton pair in our disaccharide, the angle for the cone can be estimated to 23°. For the two conformers, obtained from energy minimizations as described above, an estimate of a cone semiangle can be obtained from an overlay (least-squares fit) of the terminal mannosyl group. The semiangle θ_0 for H1′ and H3 in the two conformers is ∼16°, consistent with the experimental data and a certain degree of flexibility for the ψ dihedral angle. Thus, it is possible that two conformers are accessible.

The question of the possible barriers is more difficult. We can state that a slow motion around the glycosidic linkage, slower than the global reorientation, would not be seen in the experiments reported in this study. If the local motions and the overall reorientation were on a similar time scale, then we would expect a difference between the Lipari−Szabo global correlation times sensed by the carbon−proton and *trans*-glycosidic proton−proton vectors. The rapid motion within the accessible conformational space—corresponding to a low barrier between the low-energy conformers—would be most consistent with the Lipari−Szabo model and the way in which it successfully explains our experimental data.

Conclusions

The combined variable-field, variable-temperature carbon-13 and proton relaxation data for the monosaccharide, 1,6-anhydro-β-D-galactopyranoside, and the disaccharide, α-D-Man*p*-(1→3)-β-D-Glc*p*-OMe, are found to be internally consistent for "fixed" intra-ring proton distances, if the dynamics of the molecules is described by the Lipari−Szabo model. The results show that the internal motions must be properly taken into account in the interpretation of carbon-13 relaxation data for the carbon-13 and proton relaxation results to be compatible. The intra-ring proton cross-relaxation data, combined with the dynamics from carbon-13 measurements, lead to a reference distance in reasonable agreement with the molecular modeling. The same dynamical parameters can also explain the field and temperature dependence of an inter-ring proton cross-relaxation rate. We interpret this finding as a strong indication of the lack of rapid large-amplitude motions around the glycosidic linkage. The Lipari−Szabo order parameter and the diffusion in the cone semiangle obtained for the *trans*-glycosidic proton pair in the disaccharide are consistent with a certain degree of flexibility, preferably along the ψ dihedral angle. In the low-energy region, two conformers may be present and, in such a case, the energy barrier between them should be low.

Acknowledgment. This work has been supported by the Swedish Natural Science Research Council. We are indebted to the Swedish NMR Center for providing instrument time on the U300 and U500 spectrometers and to Dr. Toshi Nishida and Charlotta Damberg for skillful assistance with operating these instruments.

References and Notes

(1) Kay, L. E.; Torchia, D. A.; Bax, A. *Biochemistry* **1989**, *28*, 8972−8979.
(2) Palmer, A. G., III; Rance, M.; Wright, P. E. *J. Am. Chem. Soc.* **1991**, *113*, 4371−4380.
(3) Brüschweiler, R. *J. Chem Phys.* **1995**, *102*, 3396−3403.
(4) Koning, T. M. G.; Boelens, R.; van der Marel, G. A.; van Boom, J. H.; Kaptein, R. *Biochemistry* **1991**, *30*, 3787−3797.
(5) Brüschweiler, R.; Wright, P. E. *J. Am. Chem. Soc.* **1994**, *116*, 8426−8427.
(6) Brüschweiler, R.; Liao, X. B.; Wright, P. E. *Science* **1995**, *268*, 886−889.
(7) Stone, M. J.; Fairbrother, W. J.; Palmer, A. G., III; Reizer, J.; Saier, M. H., Jr.; Wright, P. E. *Biochemistry* **1992**, *31*, 4394−4406.
(8) Palmer, A. G., III; Hochstrasser, R. A.; Millar, D. P.; Rance M.; Wright, P. E. *J. Am. Chem. Soc.* **1993**, *115*, 6333−6345.
(9) Stone, M. J.; Chandrasekhar, K.; Holmgren, A.; Wright, P. E.; Dyson, J. *Biochemistry* **1993**, *32*, 426−435.
(10) Lipari, G.; Szabo, A. *J. Am. Chem. Soc.* **1982**, *104*, 4546−4559.
(11) Peng, J. W.; Wagner, G. *J. Magn. Reson.* **1992**, *98*, 308−322.
(12) McCain, D. C.; Markley, J. L. *J. Am. Chem. Soc.* **1986**, *108*, 4259−4264.
(13) McCain, D. C.; Markley, J. L. *J. Magn. Reson.* **1987**, *73*, 244−251.
(14) Braccini, I.; Michon, V.; Hervé du Penhoat, C.; Imberty, A.; Pérez, S. *Int. J. Biol. Macromol.* **1993**, *15*, 52−55.
(15) Hajduk, P. J.; Horita, D. A.; Lerner, L. E. *J. Am. Chem. Soc.* **1993**, *115*, 9196−9201.
(16) Dais, P. *Carbohydr. Res.* **1994**, *263*, 13−24.
(17) Hricovíni, M.; Torri, G. *Carbohydr. Res.* **1995**, *268*, 159−175.
(18) Lipari, G.; Szabo, A. *J. Am. Chem. Soc.* **1982**, *104*, 4559−4570.
(19) Kovacs, H.; Bagley, S.; Kowalewski, J. *J. Magn. Reson.* **1989**, *85*, 530−541.
(20) Bagley, S.; Kovacs, H.; Kowalewski, J.; Widmalm, G. *Magn. Reson. Chem.* **1992**, *30*, 733−739.
(21) Kowalewski, J.; Widmalm, G. *J. Phys. Chem.* **1994**, *98*, 28−34.
(22) Mäler, L.; Lang, J.; Widmalm, G.; Kowalewski, J. *Magn. Reson. Chem.* **1995**, *33*, 541−548.
(23) Hardy, B. J.; Egan, W.; Widmalm, G. *Int. J. Biol. Macromol.* **1995**, *17*, 149−160.
(24) Tropp, J. *J. Chem Phys.* **1980**, *72*, 6035−6043.
(25) Poppe, L.; van Halbeek, H. *J. Am. Chem. Soc.* **1992**, *114*, 1092−1094.
(26) Hricovíni, M.; Shah, R. N.; Carver, J. P. *Biochemistry* **1992**, *31*, 10018−10023.
(27) Adams, B.; Lerner, L. *J. Am. Chem. Soc.* **1992**, *114*, 4827−4829.
(28) Widmalm, G.; Venable, R. M. *Biopolymers* **1994**, *34*, 1079−1088.
(29) Dabrowski, J.; Kožár, T.; Grosskurth, H.; Nifant'ev, N. E. *J. Am. Chem. Soc.* **1995**, *117*, 5534−5539.
(30) Balling Engelsen, S.; Pérez, S.; Braccini, I.; Hervé du Penhoat, C. *J. Comput. Chem.* **1995**, *16*, 1096−1119.
(31) Shimizu, H. *J. Chem. Phys.* **1964**, *40*, 3357−3364.
(32) Brüschweiler, R.; Roux, B.; Blackledge, M.; Griesinger, C.; Karplus, M.; Ernst, R. R. *J. Am. Chem. Soc.* **1992**, *114*, 2289−2302
(33) Jansson, P.-E.; Kenne, L.; Persson, K.; Widmalm, G. *J. Chem. Soc., Perkin Trans. 1* **1990**, 591−598.
(34) Widmalm, G.; Byrd, R. A.; Egan, W. *Carbohydr. Res.* **1992**, *229*, 195−211.
(35) Canet, D.; Levy, G. C.; Peat, I. R. *J. Magn. Reson.* **1975**, *18*, 199−204.
(36) Kowalewski, J.; Ericsson, A.; Vestin, R. *J. Magn. Reson.* **1978**, *31*, 165−169.
(37) Kessler, H.; Oschkinat, H.; Griesinger, C.; Bermel, W. *J. Magn. Reson.* **1986**, *70*, 106−133.
(38) Kessler, H.; Anders, U.; Gemmecker, G.; Steuernagel, S. *J. Magn. Reson.* **1989**, *85*, 1−14.
(39) Macura, S.; Ernst, R. R. *Mol. Phys.* **1980**, *41*, 95−117.
(40) Odelius, M.; Laaksonen, A.; Widmalm, G. *J. Phys. Chem.* **1995**, *99*, 12686−12692.
(41) Mäler, L.; Widmalm, G.; Kowalewski, J. *J. Biomol. NMR* **1996**, *7*, 1−7.
(42) Noggle, J. H.; Schirmer, R. E. *The Nuclear Overhauser Effect*; Academic Press: New York, 1971.
(43) Bundle, D. R.; Baumann, H.; Brisson, J.-R.; Gagné, S. M.; Zdanov, A.; Cygler, M. *Biochemistry* **1994**, *33*, 5183−5192.
(44) Cagas, P.; Bush, C. A. *Biopolymers* **1990**, *30*, 1123−1138.
(45) Ernst, R. R.; Bodenhausen, G.; Wokaun, A. *Principles of Nuclear Magnetic Resonance in One and Two Dimensions*; Clarendon Press: Oxford, U.K., 1987.
(46) Lipari, G.; Szabo, A. *Biophys. J.* **1980**, *30*, 489−506.

JP961236L